

## RESEARCH ARTICLE

# The cell surface protein MUL\_3720 confers binding of the skin pathogen *Mycobacterium ulcerans* to sulfated glycans and keratin

Christopher J. Day<sup>1</sup>, Katharina Röltgen<sup>2,3</sup>, Gerd Pluschke<sup>2,3\*</sup>, Michael P. Jennings<sup>1\*</sup>

**1** Institute for Glycomics, Griffith University, Gold Coast, Queensland, Australia, **2** Swiss Tropical and Public Health Institute, Basel, Switzerland, **3** University of Basel, Basel, Switzerland

\* [Gerd.Pluschke@swisstph.ch](mailto:Gerd.Pluschke@swisstph.ch) (GP); [m.jennings@griffith.edu.au](mailto:m.jennings@griffith.edu.au) (MPJ)



## Abstract

*Mycobacterium ulcerans* is the causative agent of the chronic, necrotizing skin disease Buruli ulcer. Modes of transmission and molecular mechanisms involved in the establishment of *M. ulcerans* infections are poorly understood. Interactions with host glycans are often crucial in bacterial pathogenesis and the 22 kDa *M. ulcerans* protein MUL\_3720 has a putative role in host cell attachment. It has a predicted *N*-terminal lectin domain and a *C*-terminal peptidoglycan-binding domain and is highly expressed on the surface of the bacilli. Here we report the glycan-binding repertoire of whole, fixed *M. ulcerans* bacteria and of purified, recombinant MUL\_3720. On an array comprising 368 diverse biologically relevant glycan structures, *M. ulcerans* cells showed binding to 64 glycan structures, representing several distinct classes of glycans, including sulfated structures. MUL\_3720 bound only to glycans containing sulfated galactose and GalNAc, such as glycans known to be associated with keratins isolated from human skin. Surface plasmon resonance studies demonstrated that both whole, fixed *M. ulcerans* cells and MUL\_3720 show high affinity interactions with both glycans and human skin keratin extracts. This MUL\_3720-mediated interaction with glycans associated with human skin keratin may contribute to the pathobiology of Buruli ulcer.

## OPEN ACCESS

**Citation:** Day CJ, Röltgen K, Pluschke G, Jennings MP (2021) The cell surface protein MUL\_3720 confers binding of the skin pathogen *Mycobacterium ulcerans* to sulfated glycans and keratin. PLoS Negl Trop Dis 15(2): e0009136. <https://doi.org/10.1371/journal.pntd.0009136>

**Editor:** Bradley R. Borlee, Colorado State University, UNITED STATES

**Received:** September 4, 2019

**Accepted:** January 13, 2021

**Published:** February 25, 2021

**Peer Review History:** PLOS recognizes the benefits of transparency in the peer review process; therefore, we enable the publication of all of the content of peer review and author responses alongside final, published articles. The editorial history of this article is available here: <https://doi.org/10.1371/journal.pntd.0009136>

**Copyright:** © 2021 Day et al. This is an open access article distributed under the terms of the [Creative Commons Attribution License](https://creativecommons.org/licenses/by/4.0/), which permits unrestricted use, distribution, and reproduction in any medium, provided the original author and source are credited.

**Data Availability Statement:** All relevant data are within the manuscript and its [Supporting Information](#) files.

## Author summary

*Mycobacterium ulcerans* causes a skin-based disease known as Buruli ulcer. How the bacteria are transmitted and what mechanisms they use to establish the infection of the skin is poorly understood. The only well characterized bacterial factor in Buruli ulcer pathogenesis is mycolactone, a toxin produced by the bacteria. Mycolactone causes apoptosis in human cells, leading to destruction of the skin around extracellular clusters of the mycobacteria. Human cells, like cells of all orders of life, are coated in complex sugar structures and these glycans are one of the major targets of bacteria and viruses for the interaction with host cells. Here we describe the glycan binding of whole *Mycobacterium ulcerans* cells and a mycobacterial protein, MUL\_3720, thought to be involved in glycan binding. We show that both the bacterial cells and MUL\_3720 bind to glycans known to be associated with human skin keratin and to skin keratin extracts. This binding of keratin extracts

**Funding:** This work was supported by a National Health and Medical Research Council (NHMRC; <https://www.nhmrc.gov.au/>) Program Grant (1071659 to MPJ), NHMRC Principal research fellowship (APP1138466 to MPJ) and a grant of the Medicor Foundation (to GP; <https://medicor.li/en/>). The funders had no role in study design, data collection and analysis, decision to publish, or preparation of the manuscript.

**Competing interests:** The authors have declared that no competing interests exist.

may explain initial bacterial attachment and clustering of the bacteria in the skin, ultimately leading to tissue destruction and ulceration caused by a cloud of secreted mycolactone at the site of infection.

## Introduction

Buruli ulcer (BU) is a chronic, necrotizing skin disease, caused by *Mycobacterium ulcerans* [1]. It affects populations living in contact with stagnant or slow flowing water bodies primarily in West and Central Africa, but has also been reported from Asia, the Americas, Papua New Guinea and Australia [2]. The interaction of *M. ulcerans* with the human host is not fully understood. The site of inoculation of the bacteria into susceptible layers of the skin is thought to be the site where an infection is established. Presence of only one lesion in the majority of BU patients speaks for a very low rate of contiguous spread. Thermo-sensitivity of the pathogen may in part explain why infections are typically confined to the cooler surface of the body rather than internal organs, which are not infected [3]. Production of the macrolide toxin mycolactone by *M. ulcerans* [4] causes apoptosis in mammalian cells [5] and leads to extensive tissue necrosis. In advanced BU lesions, extracellular clusters [6] of the pathogen are residing in completely necrotic areas, primarily localized in deeper layers of subcutaneous fat tissue [7]. A protective cloud of mycolactone appears to prevent infiltrating leukocytes to reach the bacteria [8]. Clustering of the bacteria and skin location thus appear key elements in the long-term persistence of *M. ulcerans* in the chronically infected immunocompetent host.

Many studies indicate a key role for host carbohydrates as targets for bacterial adhesins [9]. Here we conducted a glycomic analysis to define the glycan-binding repertoire of whole, fixed *M. ulcerans* cells. In a second step, we compared this repertoire with the glycan-binding activity of the candidate adhesin MUL\_3720. 2D gel electrophoretic analysis of an *M. ulcerans* whole protein lysate has shown that MUL\_3720 is one of the most highly expressed proteins of the pathogen, a feature that is currently being exploited in the development of a diagnostic antigen capture assay [10]. The function of MUL\_3720 is suggested by its two-domain structure, with a conserved bulb-type lectin domain and a Lysine Motif (LysM) domain, which is predicted to be involved in binding to peptidoglycan [11]. Studies with a mycobacterial-specific two-hybrid system furthermore indicated that MUL\_3720 interacts with a range of cell wall associated proteins [10]. Immunofluorescence staining of *M. ulcerans* bacilli demonstrated a cell wall localization of MUL\_3720 [10,12] and all these features together suggested that MUL\_3720 plays a role in the binding of *M. ulcerans* cells to glycosylated substrates. Here we show that MUL\_3720 is binding to sulfated galactose and GalNAc structures, which are elements of sulfated glycosaminoglycans (GAGs), such as chondroitin sulfate, dermatan sulfate and heparan sulfate.

## Materials and methods

### Growth and maintenance of *M. ulcerans*

The *M. ulcerans* strain S1013, recently isolated from the lesion of a BU patient from Cameroon [13] was grown in BacT/Alert culture bottles supplemented with enrichment medium according to the manufacturer's protocol (bioMérieux). Cells were fixed with 4% formalin prior to array and SPR analysis.

### Cloning, expression, and purification of MUL\_3720

Full length MUL\_3720 (aa 1–207) was cloned into pET28a, as previously outlined [14]. The recombinant protein was expressed and purified as previously described [10,14], with the purity on par with that shown in Bolz *et al.* 2016 [14].

### Evolutionary analysis of the MUL\_3720 protein

The MUL\_3720 protein sequence was analysed using the BLAST tool (NCBI) against the non-redundant protein sequence database and mycobacterial sequences with an e-value of  $> 1e-30$  were downloaded for further analysis against the MUL\_3720 sequence. The evolutionary history of the retrieved sequences was inferred using the Maximum Likelihood method and Whelan And Goldman + Freq. model [15]. Initial tree(s) for the heuristic search were obtained automatically by applying Neighbour-Join and BioNJ algorithms to a matrix of pairwise distances estimated using a JTT model, and then selecting the topology with superior log likelihood value. A discrete Gamma distribution was used to model evolutionary rate differences among sites (5 categories (+G, parameter = 0.5861)) of an 88 amino acid sequence region of the proteins. Evolutionary analyses were conducted in MEGA X [16,17] and shown in S1 Fig.

### Glycan array analysis

Glycan arrays were printed onto SuperEpoxy 3 activated substrates as previously described [18]. The glycan array analysis of the whole, fixed *M. ulcerans* cells was performed using a modification of the method used in Day *et al.* 2009 and Mubaiwa *et al.* 2017 [19,20]. Briefly, approximately  $10^6$  Bodipy 595/625 nm labelled bacteria in 500  $\mu$ L of array PBS (1 x PBS containing 1 mM  $\text{CaCl}_2$  and 1 mM  $\text{MgCl}_2$ ) were applied to the glycan array in a 65  $\mu$ L gene frame without a cover. The bacteria were incubated on the array at room temperature in the dark for 30 minutes and washed three times for five minutes, once in array PBS and twice in 1x PBS without Mg or Ca ions. Glycan arrays with the MUL\_3720 protein were performed as previously described [21] using 2  $\mu$ g of protein per array and 20 minutes of incubation time prior to washing. Both protein and cell arrays were scanned and analysed using the Innoscan 1100AL scanner and the MAPIX analysis package. Final statistical analysis of the combined datasets were performed in Microsoft Excel using Student's T test. The list of glycans is present in S1 Data and the MIRAGE compliance information is included in S1 Table.

### Surface plasmon resonance analysis

Surface plasmon resonance (SPR) analyses were performed as previously described on a Biacore T200 using a Series S C1 chip for whole bacteria analysis [20,22] and a CM5 chip for protein analysis [21] with the following modifications. Proteins were immobilized onto a CM5 chip at pH 4.5, flow rate of 5  $\mu$ L/min for 600 seconds with an ethanolamine blank flow cell as a control. The C1 chip was prepared as per manufacturer's instructions and 100  $\mu$ L of bacteria at approximately  $10^6$  cells per mL at pH 4.5 were immobilized using amine chemistry at a flow rate of 5  $\mu$ L per minute for 720 seconds. Glycans (Fuc $\alpha$ 1-2Gal, Fuc $\alpha$ 1-2Gal $\beta$ 1-4(Fuc $\alpha$ 1-3)GlcNAc, Neu5Ac $\alpha$ 2-6Gal $\beta$ 1-4GlcNAc, Fuc $\alpha$ 1-2(3-O-Su)Gal $\beta$ 1-3(Fuc $\alpha$ 1-4)GlcNAc; Elicityl, mannose glycans; Dextra Laboratories), GAGs (GAGs; Dextra Laboratories) and keratin isolated from human epidermis (mixed keratins with average molecular weight of 64.1 kDa; Sigma-Aldrich, Cat# K0253) were tested between 2 nM and 20  $\mu$ M. All data was double reference subtracted. Analysis was performed using the Biacore T200 Evaluation software package. Competition assays were performed using the sulphated chondroitin disaccharide  $\Delta$ UA $\alpha$ 1-3GalNAc-6S and a keratin extract, which were flowed separately or together at a maximum of

10 times the calculated  $K_D$  ( $1\mu\text{M}$  for  $\Delta\text{UA}\alpha\text{1-3GalNAc-6S}$  and  $50\text{nM}$  for keratin extract) to ensure saturation in direct competition using a modification of a previously described method [20]. Maximum responses for each interaction were used as final point data for the interaction and compared to the calculated average and addition to determine the presence of a shared or separate binding site.

### **N-linked glycan endoglycosidase PNGase F treatment of keratin from human epithelial cells**

Keratin isolated from human epidermis (10  $\mu\text{g}$  mixed keratins with average molecular weight of 64.1 kDa; Sigma-Aldrich, Cat# K0253) was treated with PNGase F (New England Biolabs) under denaturing conditions as described in the manufacturers protocol. The same quantity of keratin was incubated in the same buffers for the same time without PNGase F as a control. Half of each reaction, plus/minus PNGase, were run on 4–12% PAGE gels in duplicate and the gels were cut in half and stained using different methods. One gel half was stained with the ProteoSilver Silver Stain Kit (Sigma) following manufacturers protocol for the staining of proteins. The other portion of the gel was stained using the ProteoSilver Silver Stain Kit (Sigma) following the method for the staining of sugars as previously described [23]. A DNA ladder was run as a control for the sugar staining and a NEB 11-250kDa prestained blue protein ladder was run as a control for the protein size and staining.

## **Results**

### ***M. ulcerans* cells and MUL\_3720 bind to a subset of sulfated glycans**

MUL\_3720 is annotated as a possible lectin, based on the presence of a B-lectin domain that has a mannose binding consensus sequence [10], to our knowledge the only annotated lectin in *M. ulcerans*. Due to this hypothesised lectin activity, both MUL\_3720 and whole fixed *M. ulcerans* cells were analysed for glycan binding activity using a glycan arrays. This analysis revealed that the *M. ulcerans* cells bind to 64 of the 368 glycans printed on the array (Table 1 and S1 Data). We reasoned that MUL\_3720 may be responsible for part of these interactions and found that it is binding to seven glycans on the array (Table 1, S1 Data). The *M. ulcerans* cells bound to a range of distinct glycans including mannose structures, Lewis and ABO blood group antigens, sialylated glycans and sulfated glycans including both sulphated GAGs and sulfated galactose and GalNAc structures (Table 1). MUL\_3720 only recognized sulfated galactose and GalNAc structures including those typical of the glycosylation present on keratins and GAGs (Table 1) [24–26].

### ***M. ulcerans* cells and MUL\_3720 bind to specific glycans with high affinity**

To validate the glycan array results using a different technique and to determine the dissociation equilibrium constant ( $K_D$ ) of the interactions, SPR analyses were performed between free oligosaccharides and *M. ulcerans* cells or purified recombinant MUL\_3720 that were bound to sensor chips (Table 2). Eight glycan structures representative for each of the distinct glycan groups that either bound only to *M. ulcerans* cells or to both *M. ulcerans* cells and purified MUL\_3720 were chosen. These structural groups are representatives of blood group antigens (Fuc $\alpha$ 1-2Gal), Lewis antigens (Fuc $\alpha$ 1-2Gal $\beta$ 1-4(Fuc $\alpha$ 1-3)GlcNAc), sulfated glycans (GAGs including chondroitin 6S-complex polymer, chondroitin 62 disaccharide  $\Delta\text{UA}\alpha$  1-3GalNAc-6S and, heparin and Fuc $\alpha$ 1-2(3-O-Su)Gal $\beta$ 1-3(Fuc $\alpha$ 1-4)GlcNAc), mannose structures (Man $\alpha$ 1-3Man, Man $\alpha$ 1-6(Man $\alpha$ 1-3)Man $\alpha$ 1-6(Man $\alpha$ 1-3)Man) and sialylated glycans (Neu5Ac $\alpha$ 2-6Gal $\beta$ 1-4GlcNAc). This set of structures provides a broad coverage of the glycan

**Table 1. Glycans bound by *M. ulcerans* cells and MUL\_3720 protein in glycan array analysis.** Red labelling indicates binding as determined by interaction above background in three replicate array experiments. A positive fluorescent value is defined as any value above the average background fluorescence of 20 negative control spots + 3 standard deviations. Data are presented as fold-above this background value, which were 2706±372 RFU for *M. ulcerans* cells and 1829±140 RFU for the MUL\_3720 studies. Only glycans that showed binding are shown; see S1 Data for full array results and list of all the glycans present on the array.

Array ID	Structure	<i>M. ulcerans</i>	MUL_3720
<b>Terminal Galactose Structures</b>			
145	Galβ1-3(6-O-Su)GlcNAcβ-sp3	1.92±0.64	0.432099
146	Galβ1-4(6-O-Su)Glcβ-sp2	1.59±0.18	0.382383
147	Galβ1-4(6-O-Su)GlcNAcβ-sp3	1.94±0.34	0.441459
151	6-O-Su-Galβ1-3GalNAcα-sp3	1.87±0.40	2.44±0.88
152	3-O-Su-Galβ1-4Glcβ-sp2	1.91±0.98	0.432046
159	4-O-Su-Galβ1-4GlcNAcβ-sp3	1.73±0.26	0.234259
161	6-O-Su-Galβ1-3GlcNAcβ-sp3	1.64±0.37	2.49±0.26
178	6-O-Su-Galβ1-4(6-O-Su)Glcβ-sp2	1.17±0.26	0.442476
179	6-O-Su-Galβ1-3(6-O-Su)GlcNAcβ-sp2	1.60±0.41	1.48±0.33
180	6-O-Su-Galβ1-4(6-O-Su)GlcNAcβ-sp2	1.83±0.51	0.456808
182	3,6-O-Su <sub>2</sub> -Galβ1-4GlcNAcβ-sp2	1.99±0.62	3.29±1.77
189	3,6-O-Su <sub>2</sub> -Galβ1-4(6-O-Su)GlcNAcβ-sp2	1.90±0.45	2.46±0.56
201	3,4-O-Su <sub>2</sub> -Galβ1-4GlcNAcβ-sp3	1.92±0.92	1.52±0.64
203	Galβ1-4(6-O-Su)GlcNAcβ-sp2	1.92±0.79	0.457048
18C	Galβ1-3GalNAcβ1-3Gal	1.77±0.94	0.488285
<b>Fucosylated glycans</b>			
215	Fucα1-2Galβ1-3GlcNAcβ-sp3	1.86±0.26	0.361827
219	Fucα1-2Galβ1-4Glcβ-sp4	1.88±0.93	0.42071
542	Le <sup>c</sup> Le <sup>x</sup> 1-6'(Le <sup>c</sup> 1-3')Lac-sp4	2.77±0.76	0.045969
7A	Fucα1-2Galβ1-3GlcNAcβ1-3Galβ1-4Glc	1.63±0.92	0.325579
7E	Galβ1-3(Fucα1-4)GlcNAcβ1-3Galβ1-4(Fucα1-3)Glc	1.82±0.72	0.459277
7G	Fucα1-2Galβ1-4Glc	1.69±0.59	0.444367
7L	Fucα1-2Galβ1-4(Fucα1-3)Glc	1.83±0.80	0.471871
7P	Fucα1-2Galβ1-3(Fucα1-4)GlcNAc	1.66±0.26	0.473629
<b>Terminal N-Acetylgalactosamine</b>			
4	GalNAcα-sp0	1.48±0.63	0.392032
193	3-O-Su-GalNAcβ1-4GlcNAcβ-sp3	1.52±0.95	0.261001
195	6-O-Su-GalNAcβ1-4-(3-O-Su)GlcNAcβ-sp3	1.93±0.86	0.409689
199	4,6-O-Su <sub>2</sub> -GalNAcβ1-4-(3-O-Ac)GlcNAcβ-sp3	1.54±0.79	2.45±0.87
2C	GalNAcβ1-3Gal	1.76±0.40	0.414296
2F	GalNAcα1-3Galβ1-4Glc	1.89±0.34	0.557756
<b>Mannose</b>			
19	ManNAcβ-sp4	1.72±0.45	0.357543
5D	Manα1-3Man	1.48±0.34	0.022
5E	Manα1-4Man	1.56±0.81	0.213395
119	Manα1-2Manβ-sp4	1.49±0.14	0.481129
122	Manα1-6Manβ-sp4	1.49±0.28	-0.02186
123	Manβ1-4GlcNAcβ-sp4	1.69±0.54	0.47481
<b>N-Acetylglucosamine</b>			
118	GlcNAcβ1-6GalNAcα-sp3	1.67±0.81	0.107263
149	GlcNAcβ1-4(6-O-Su)GlcNAcβ-sp2	1.68±0.29	-0.0567
493	(GlcNAcβ1-4) <sub>5</sub> β-sp4	1.47±0.32	0.24036
4C	GlcNAcβ1-4GlcNAcβ1-4GlcNAcβ1-4GlcNAc	1.44±0.59	0.137314
4E	GlcNAcβ1-4MurNAc	1.48±0.73	0.04918

(Continued)

Table 1. (Continued)

Array ID	Structure	<i>M. ulcerans</i>	MUL_3720
18G	6-O-Su-GlcNAc	1.30±0.675	0.441581
<b>N-Acetylneuraminic acid</b>			
18K	9-NAc-Neu5Ac	1.99±0.46	0.494373
18O	Neu5Gc	1.60±0.59	0.464909
169	Neu5Ac $\alpha$ 2-3Gal $\beta$ -sp3	1.70±0.31	0.327169
170	Neu5Ac $\alpha$ 2-6Gal $\beta$ -sp3	1.77±0.18	0.516095
171	Neu5Ac $\alpha$ 2-3GalNAc $\alpha$ -sp3	1.51±0.70	0.41582
172	Neu5Ac $\alpha$ 2-6GalNAc $\alpha$ -sp3	1.68±0.34	0.470861
174	Neu5Gc $\alpha$ 2-6GalNAc $\alpha$ -sp3	1.77±0.24	0.469814
421	GalNAc $\beta$ 1-4(Neu5Ac $\alpha$ 2-3)Gal $\beta$ 1-4Glc $\beta$ -sp2	1.83±0.41	0.469452
533	GalNAc $\beta$ 1-4(Neu5Ac $\alpha$ 2-8Neu5Ac $\alpha$ 2-8Neu5Ac $\alpha$ 2-3)Gal $\beta$ 1-4Glc-sp2	1.62±0.77	0.468232
<b>Glucose</b>			
9	Glc $\beta$ -sp3	1.63±0.71	0.457861
164	GlcA $\beta$ 1-3GlcNAc $\beta$ -sp3	1.52±0.48	-0.03734
165	GlcA $\beta$ 1-3Gal $\beta$ -sp3	1.45±0.40	0.137664
166	GlcA $\beta$ 1-6Gal $\beta$ -sp3	1.61±0.36	0.09887
18J	6-H <sub>2</sub> PO <sub>3</sub> Glc	1.40±0.88	0.480741
<b>Glycosaminoglycans</b>			
12A	Neocarratetrose-41, 3-di-O-sulphate (Na <sup>+</sup> )	1.63±0.86	0.143975
12B	Neocarratetrose-41-O-sulphate (Na <sup>+</sup> )	1.69±0.81	0.217521
12E	Neocarraoctose-41, 3, 5, 7-tetra-O-sulphate (Na <sup>+</sup> )	1.67±0.91	0.102244
12G	$\Delta$ UA-2S-GlcNS-6S Na <sub>4</sub> (I-S)	1.41±0.78	0.198534
12M	$\Delta$ UA-GlcNAc Na (IV-A)	1.73±0.60	0.249342
13K	Chondroitin sulfate	2.71±1.74	0.836093
13L	Dermatan sulfate	2.70±0.58	0.852452
13N	HA—4	1.79±0.64	0.622733
14I	HA 1600000 Da	2.67±0.94	0.846553

<https://doi.org/10.1371/journal.pntd.0009136.t001>

types recognised by both *M. ulcerans* cells and purified MUL\_3720 to aid in the identification of the hierarchy of glycan recognition. The SPR analyses reconfirmed that both MUL\_3720 and *M. ulcerans* cells interact with high affinity ( $K_D$  in the low  $\mu$ M range) with sulfated glycans and GAGs (Table 2).

In the SPR analysis, MUL\_3720 showed the strongest binding to the chondroitin 6S-disaccharide  $\Delta$ UA $\alpha$  1-3GalNAc-6S. However, due to lack of availability, the best MUL\_3720 binding glycans from the array analysis (compounds 151, 161, 182, 189 and 199) were not analysed. There is a large difference between the complex 6S-polymer and the 6S-disaccharide of chondroitin, with a greater than 10-fold higher affinity to the 6S-disaccharide for both the *M. ulcerans* cells and MUL\_3720. The binding to  $\alpha$ 2-6 sialylated glycans on the glycan array were confirmed to be differential between *M. ulcerans* cells and MUL\_3720 with the whole bacteria binding to the  $\alpha$ 2-6Neu5Ac terminating glycan (Neu5Ac $\alpha$ 2-6Gal $\beta$ 1-4GlcNAc) with ~4600-fold higher affinity than MUL3720 (Table 2).

### ***M. ulcerans* cells and MUL\_3720 show high affinity interactions with human keratin extract**

Reports studying keratins isolated from primary human cells rather than cancer cell lines, have reported the presence of keratan sulfate glycans in human keratin extracts [26]. Due to this



**Table 2. SPR results for the binding of *M. ulcerans* cells and MUL\_3720 protein to selected glycans.** Shown are dissociation equilibrium constants ( $K_D$ ) of the interactions between free oligosaccharides and captured *M. ulcerans* cells and MUL\_3720 protein; NCDI: no concentration-dependent interaction detected up to a maximum concentration of 20  $\mu$ M. See [S2 Data](#) for representative sensorgrams.

Oligosaccharide/glycoprotein	<i>M. ulcerans</i>	MUL_3720
Fuc $\alpha$ 1-2Gal	1.10 $\mu$ M $\pm$ 0.23	NCDI
Fuc $\alpha$ 1-2Gal $\beta$ 1-4(Fuc $\alpha$ 1-3)GlcNAc	4.47 $\mu$ M $\pm$ 0.62	NCDI
chondroitin 6S (ave mol weight 14kDa)	1.93 $\mu$ M $\pm$ 0.44	4.68 $\mu$ M $\pm$ 0.75
chondroitin 6S-disaccharide $\Delta$ UA $\alpha$ 1-3GalNAc-6S	171 nM $\pm$ 28	99.2 nM $\pm$ 35
heparin (ave mol weight 14kDa)	1.48 $\mu$ M $\pm$ 0.19	1.29 $\mu$ M $\pm$ 0.078
Neu5Ac $\alpha$ 2-6Gal $\beta$ 1-4GlcNAc	1.49 nM $\pm$ 0.36	6.90 $\mu$ M $\pm$ 3.2
Fuc $\alpha$ 1-2(3-O-Su)Gal $\beta$ 1-3(Fuc $\alpha$ 1-4)GlcNAc	12.8 $\mu$ M $\pm$ 3.7	17.4 $\mu$ M $\pm$ 1.9
Man $\alpha$ 1-3Man	49.8 nM $\pm$ 11	NCDI
Man $\alpha$ 1-6(Man $\alpha$ 1-3)Man $\alpha$ 1-6(Man $\alpha$ 1-3)Man	962 nM $\pm$ 90	NCDI
Human keratin extract (ave mol weight 63kDa)	37.9 nM $\pm$ 12	4.78 nM $\pm$ 1.1

<https://doi.org/10.1371/journal.pntd.0009136.t002>

observation, we analysed the interaction of keratin extracted from human epidermis (mixed keratins with average molecular weight of 64.1 kDa) with MUL\_3720 and *M. ulcerans* cells. The cells bound to the keratin extract with a  $K_D$  of 37.9 nM (Table 2), on par with interactions observed for the glycans Neu5Ac $\alpha$ 2-6Gal $\beta$ 1-4GlcNAc and Man $\alpha$ 1-3Man. MUL\_3720 showed a nearly 10 fold higher affinity to the keratin extract ( $K_D$  4.78 nM; Table 2). To determine whether the binding of MUL\_3720 to keratin was via the sulfated N-linked glycans, we enzymatically removed N-linked glycosylation from the human keratin extract. After PNGase F treatment of the keratin extract we compared the staining using silver staining of glycans (S2 Fig lanes 3 and 4) and protein (S2 Fig lanes 6 and 7); this analysis shows that the keratin extract comprises a heterogeneous mixture of this glycoprotein, ranging from 26-43kDa. Treatment with the PNGase F removed all N-glycans leaving a single main band of reduced molecular mass. To confirm that the glycosylated portion of the keratin extract was the target for MUL\_3720 we conducted competition studies between MUL\_3720,  $\Delta$ UA $\alpha$  1-3GalNAc-6S and keratin in SPR studies (Fig 1). These data indicate strongly for an overlap of the binding sites for the 6S-disaccharide and the keratin extract, as the data for the binding to the combined ligands was closer to a combined average than to an additive signal or to one outcompeting the other.

## Discussion

We observed that *M. ulcerans* cells bind to a far smaller group of glycans present on our glycan array than other bacteria that have been assayed previously, including *Campylobacter jejuni* and *Neisseria meningitidis* [19,20]. The glycan-binding profile of *M. ulcerans* demonstrated that this skin pathogen recognises a range of negatively charged glycans common to sulfated GAGs, sialoglycoconjugates and keratans. Much of the binding is to negatively charged modifications (sulfation/sialylation) of carbon-6 of Gal or GalNAc. The whole *M. ulcerans* cells were found in SPR analyses to have the highest affinity among the tested glycans for the sialylated Neu5Ac $\alpha$ 2-6Gal $\beta$ 1-4GlcNAc (Table 2). While this exact glycan was not bound on the array, smaller mono/disaccharide versions of it were tested on the array. Testing using the larger free trisaccharide can reflect the results of smaller sugars. This is due to the flexibility of a glycan that has not been anchored on the non-reducing end, the end normally attached to a protein/lipid/array surface. The non-reducing GlcNAc of this sugar is not in any fixed anomeric configuration ( $\alpha/\beta$ ) due to it not being linked. All the glycans on the array have a fixed anomeric configuration and orientation dictated by the linkage to the spacer. This spacer effect

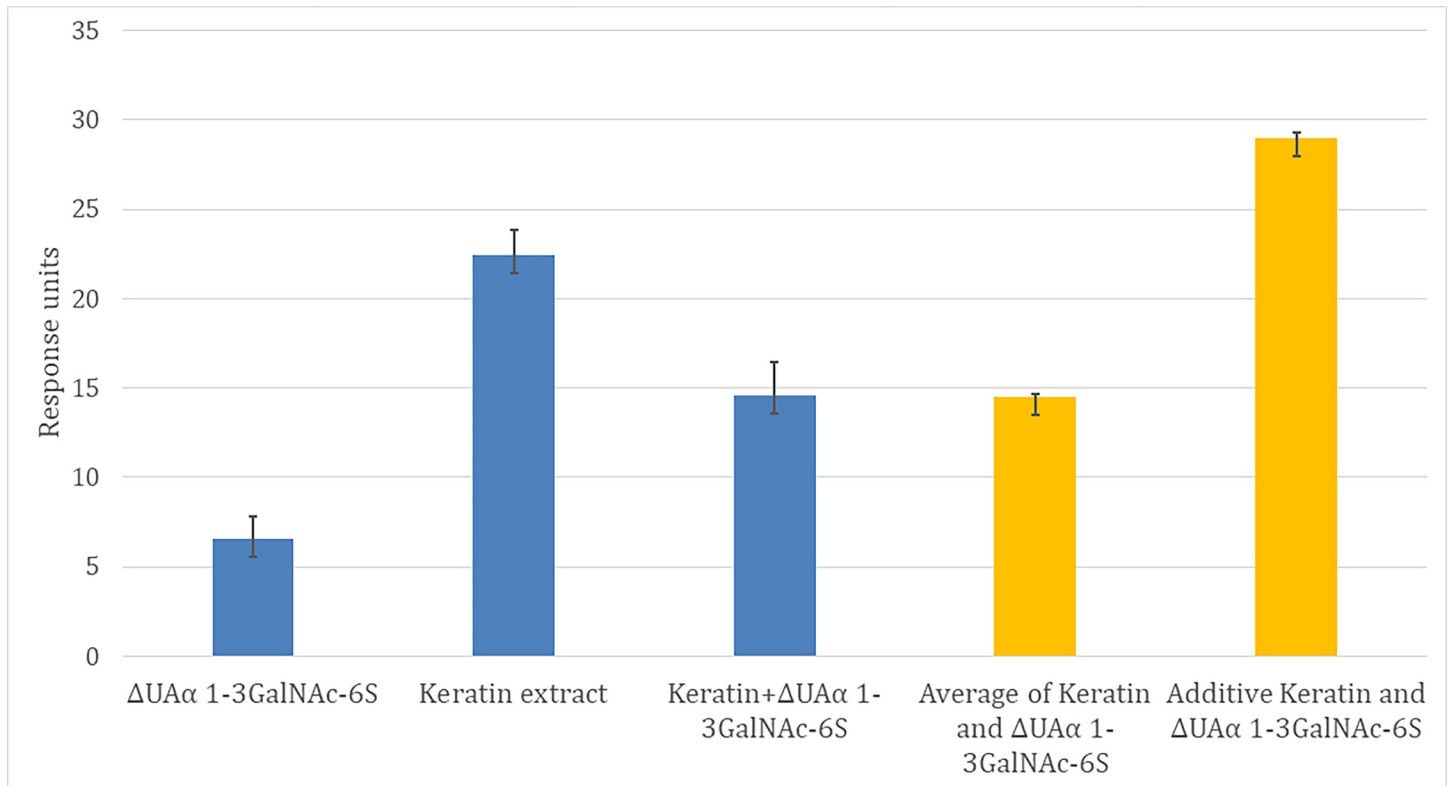


**Fig 1. SPR competition analysis of  $\Delta$ UA $\alpha$  1-3GalNAc-6S and keratin extract.** Values are the average maximum endpoint response units obtained individually and in competition at  $10\times K_D$ . The two columns in orange represent the expected values for either a shared binding site (average signal for keratin and  $\Delta$ UA $\alpha$  1-3GalNAc-6S) or separate binding sites (additive signal for keratin and  $\Delta$ UA $\alpha$  1-3GalNAc-6S).

<https://doi.org/10.1371/journal.pntd.0009136.g001>

has been observed to effect the binding of molecules to glycans printed on arrays previously [27,28]. It is due to the effect of presentation that testing with a second method such as SPR is so important. In human skin Neu5Ac $\alpha$ 2–6 is known to be associated with eccrine sweat glands [29], which may be a potential invasion site for *M. ulcerans* [30]. The high affinity binding of this structure was not due to MUL\_3720, and is likely to be mediated by another *M. ulcerans* lectin.

Furthermore, the bacilli also bind to mannose structures, which are a major component of *N*-linked glycans [31]. Mannose glycans play an important role in the skin, with mannose-containing *N*-linked glycans important for skin homeostasis cell-cell adhesion and cell motility [32,33]. The surface expression of mannose-containing *N*-linked glycans on cells of the skin may provide an initial attachment site for *M. ulcerans*, but the bacterial surface factors involved in this binding remain to be determined.

Mycobacterial species produce numerous cell surface glycan structures with a large proportion of their surface glycosylation being lipid-linked sugars. Recently, glycan-glycan interactions have been identified as a mechanism for pathogen association with host cells [9,20,34–37]. Surface glycans such as the lipo-oligo/polysaccharide of Gram-negative bacteria have been shown to bind to host surface glycans [9,34,35,38,39]. The extent and diversity of the glycolipids produced by mycobacterial species may thus provide another adherence factor that can explain the glycan recognition of *M. ulcerans* cells in the glycan array experiment.

The *M. ulcerans* protein MUL\_3720 recognises a subset of the determined *M. ulcerans* glycan binding profile, including sulfated galactose and sulfated GalNAc structures. These



sulfated glycans are primarily found as components of the GAGs chondroitin (repeating GalNAc( $\pm 2,4,6S$ ) $\beta 1-3GlcA$ ), dermatin (repeating GalNAc( $\pm 2,4,6S$ ) $\beta 1-3IdoA$ ) and as keratan sulfate glycosylations. Keratan sulfate glycans come in a range of forms including GalNAc $\alpha$ ( $\pm 3,6S$ ) $1-3Gal(NAc(\pm 6S)\beta$  [25], Gal( $\pm 6S$ ) $\beta 1-3GlcNAc(\pm 6S)/GalNAc(\pm 6S)$  [24,26], and keratan sulfate glycans containing Gal( $\pm 6S$ ) $\beta 1-3GlcNAc(\pm 6S)/GalNAc(\pm 6S)$ , present on proteins including lumican, keratocan, and mimecan. The MUL\_3720 protein was predicted to be a mannose binding lectin [10], however, the glycan array analysis revealed that MUL\_3720 is binding to sulphated GAGs and not to mannose structures. MUL\_3720 is an orthologue of a predicted lectin found in multiple other mycobacterial species including *M. marinum*, *M. basiliense*, *M. riyadhense*, *M. attenuatum*, *M. gastri*, *M. pseudokansasii*, *M. innocens* and *M. persicum*, with the *M. marinum* orthologue being most similar (99% sequence identity [10]) to the *M. ulcerans* protein (S1 Fig). Like *M. ulcerans*, *M. marinum* infections in humans are also typically limited to the skin [40–43], indicating the possibility that *M. marinum* MMAR\_3773 is targeting similar glycans. *M. marinum* also causes a tuberculosis like infection in various fish species [40] and sulphated GalNAc structures such as those found in keratan and chondroitin sulfate are the most common sulfated GAGs in many fish species [44–46]. The data on MUL\_3720 may be indicative for a role of MMAR\_3773 in *M. marinum* infections in both humans and fish.

*M. ulcerans* infects skin, one of the keratin/keratan-rich tissues of the body, with the epidermal layer being made of keratinocytes and the dermal layer having high keratan sulfate areas around hair follicles and sweat glands/ducts [47,48]. Furthermore, human skin keratin extracts have indicated that keratin is either strongly associated with or is decorated by keratan sulfate glycosylation [26] (S2 Fig). Keratan sulfate proteoglycans such as lumican are crucial components of the dermal layer of skin [49,50]. Mice lacking lumican have skin laxity and fragility caused by improper organisation of collagen fibrils [49]. Keratin and keratan sulfate-containing proteins have a wide range of functions throughout the body, including intimate involvement in wound healing [24,47,50–52]. MUL\_3720 binds with high affinity ( $K_D = 4.78$  nM) to keratin and this binding may have a role in adherence, tissue tropism, and the formation of extracellular clusters of the pathogen in the skin. Clustering of the bacteria appears to be a prerequisite for the formation of a protective cloud of mycolactone that prevents elimination of the bacteria by phagocytes [8]. Most BU patients have only a single lesion and formation of satellite lesions is rare. This is indicative for retention of the bacteria to the infected skin area and the abundant protein MUL\_3720 may play an important role in tissue tropism and sequestration.

## Supporting information

**S1 Data. Red indicates binding.** Binding is determined by positive interaction in three replicate array experiments. Positive interactions are determined by a background subtracted fluorescence value significantly above background subtracted fluorescence of negative control spots (average background fluorescence from 20 spots + 3 standard deviations).  
(PDF)

**S2 Data. Representative sensorgrams of SPR analysis.**  
(PDF)

**S1 Table. Supplementary glycan microarray document based on MIRAGE guidelines DOI: [10.1093/glycob/cww118](https://doi.org/10.1093/glycob/cww118).**  
(DOCX)

**S1 Fig. Evolutionary analysis of mycobacterial MUL\_3720 orthologues.**  
(TIF)

**S2 Fig. SDS-PAGE analysis of PNGase F treatment of keratin extract.** Lane 1 DNA ladder, Lane 2 and 5 NEB prestained blue protein ladder. Lane 3 and 6 Keratin extract without PNGaseF treatment. Lane 4 and 7 Keratin extract with PNGase F treatment. PNGase is labelled on the right side of the gel image.  
(TIF)

## Author Contributions

**Conceptualization:** Christopher J. Day, Katharina Röltgen, Gerd Pluschke, Michael P. Jennings.

**Data curation:** Christopher J. Day.

**Formal analysis:** Christopher J. Day, Gerd Pluschke.

**Funding acquisition:** Gerd Pluschke, Michael P. Jennings.

**Investigation:** Christopher J. Day.

**Methodology:** Christopher J. Day, Katharina Röltgen, Gerd Pluschke, Michael P. Jennings.

**Resources:** Katharina Röltgen.

**Supervision:** Michael P. Jennings.

**Writing – original draft:** Christopher J. Day, Gerd Pluschke, Michael P. Jennings.

**Writing – review & editing:** Christopher J. Day, Katharina Röltgen, Gerd Pluschke, Michael P. Jennings.

## References

1. Pluschke G, Röltgen K, editors. Buruli ulcer: *Mycobacterium ulcerans* disease. 1 ed: Springer International Publishing; 2019.
2. Röltgen K, Pluschke G. Epidemiology and disease burden of Buruli ulcer: a review. Res Rep Trop Med. 2015; 6:59–73. <https://doi.org/10.2147/RRTM.S62026>
3. Junghanss T, Johnson RC, Pluschke G. *Mycobacterium ulcerans* disease. Manson's Tropical diseases. 23rd ed. Edinburgh: Saunders Ltd; 2014. p. 519–31.
4. George KM, Chatterjee D, Gunawardana G, Welty D, Hayman J, Lee R, et al. Mycolactone: a polyketide toxin from *Mycobacterium ulcerans* required for virulence. Science 1999; 283(5403):854–7. <https://doi.org/10.1126/science.283.5403.854> PMID: 9933171.
5. Bieri R, Scherr N, Ruf MT, Dangy JP, Gersbach P, Gehringer M, et al. The Macrolide Toxin Mycolactone Promotes Bim-Dependent Apoptosis in Buruli Ulcer through Inhibition of mTOR. ACS chemical biology. 2017; 12(5):1297–307. <https://doi.org/10.1021/acscchembio.7b00053> PMID: 28294596.
6. Rondini S, Horsfield C, Mensah-Quainoo E, Junghanss T, Lucas S, Pluschke G. Contiguous spread of *Mycobacterium ulcerans* in Buruli ulcer lesions analysed by histopathology and real-time PCR quantification of mycobacterial DNA. J Pathol 2006; 208(1):119–28. <https://doi.org/10.1002/path.1864> PMID: 16261539.
7. Ruf MT, Bolz M, Vogel M, Bayi PF, Bratschi MW, Sopho GE, et al. Spatial Distribution of *Mycobacterium ulcerans* in Buruli Ulcer Lesions: Implications for Laboratory Diagnosis. PLoS neglected tropical diseases. 2016; 10(6):e0004767. <https://doi.org/10.1371/journal.pntd.0004767> PMID: 27253422; PubMed Central PMCID: PMC4890796.
8. Ruf MT, Steffen C, Bolz M, Schmid P, Pluschke G. Infiltrating leukocytes surround early Buruli ulcer lesions, but are unable to reach the mycolactone producing mycobacteria. Virulence 2017; 8(8):1918–26. <https://doi.org/10.1080/21505594.2017.1370530> PMID: 28873327; PubMed Central PMCID: PMC5810495.

9. Poole J, Day CJ, von Itzstein M, Paton JC, Jennings MP. Glycointeractions in bacterial pathogenesis. *Nat Rev Microbiol* 2018; 16(7):440–52. <https://doi.org/10.1038/s41579-018-0007-2> PMID: 29674747.
10. Dreyer A, Roltgen K, Dangy JP, Ruf MT, Scherr N, Bolz M, et al. Identification of the *Mycobacterium ulcerans* protein MUL\_3720 as a promising target for the development of a diagnostic test for Buruli ulcer. *PLoS neglected tropical diseases*. 2015; 9(2):e0003477. <https://doi.org/10.1371/journal.pntd.0003477> PMID: 25668636; PubMed Central PMCID: PMC4344477.
11. Buist G, Steen A, Kok J, Kuipers OP. LysM, a widely distributed protein motif for binding to (peptido)glycans. *Mol Microbiol* 2008; 68(4):838–47. <https://doi.org/10.1111/j.1365-2958.2008.06211.x> PMID: 18430080.
12. A V, N S, MT R, K R, G P. Localization of Mycobacterial Antigens by Immunofluorescence Staining of Agarose Embedded Cells. *J Mycobac Dis*. 2014; 4(3):150. <https://doi.org/10.4172/2161-1068.1000150>
13. Bratschi MW, Bolz M, Grize L, Kerber S, Minyem JC, Um Boock A, et al. Primary cultivation: factors affecting contamination and *Mycobacterium ulcerans* growth after long turnover time of clinical specimens. *BMC infectious diseases*. 2014; 14:636. <https://doi.org/10.1186/s12879-014-0636-7> PMID: 25433390; PubMed Central PMCID: PMC4264541.
14. Bolz M, Benard A, Dreyer AM, Kerber S, Vettiger A, Oehlmann W, et al. Vaccination with the Surface Proteins MUL\_2232 and MUL\_3720 of *Mycobacterium ulcerans* Induces Antibodies but Fails to Provide Protection against Buruli Ulcer. *PLoS neglected tropical diseases*. 2016; 10(2):e0004431. Epub 2016/02/06. <https://doi.org/10.1371/journal.pntd.0004431> PMID: 26849213; PubMed Central PMCID: PMC4746116.
15. Whelan S, Goldman N. A general empirical model of protein evolution derived from multiple protein families using a maximum-likelihood approach. *Mol Biol Evol* 2001; 18(5):691–9. Epub 2001/04/25. <https://doi.org/10.1093/oxfordjournals.molbev.a003851> PMID: 11319253.
16. Stecher G, Tamura K, Kumar S. Molecular Evolutionary Genetics Analysis (MEGA) for macOS. *Mol Biol Evol* 2020. Epub 2020/01/07. <https://doi.org/10.1093/molbev/msz312> PMID: 31904846.
17. Kumar S, Stecher G, Li M, Knyaz C, Tamura K. MEGA X: Molecular Evolutionary Genetics Analysis across Computing Platforms. *Mol Biol Evol*. 2018; 35(6):1547–9. Epub 2018/05/04. <https://doi.org/10.1093/molbev/msy096> PMID: 29722887; PubMed Central PMCID: PMC5967553.
18. Waespy M, Gbem TT, Elenschneider L, Jeck AP, Day CJ, Hartley-Tassell L, et al. Carbohydrate Recognition Specificity of Trans-sialidase Lectin Domain from *Trypanosoma congolense*. *PLoS Negl Trop Dis*. 2015; 9(10):e0004120. Epub 2015/10/17. <https://doi.org/10.1371/journal.pntd.0004120> PMID: 26474304; PubMed Central PMCID: PMC4608562.
19. Day CJ, Tiralongo J, Hartnell RD, Logue CA, Wilson JC, von Itzstein M, et al. Differential carbohydrate recognition by *Campylobacter jejuni* strain 11168: influences of temperature and growth conditions. *PLoS One*. 2009; 4(3):e4927. Epub 2009/03/18. <https://doi.org/10.1371/journal.pone.0004927> PMID: 19290056; PubMed Central PMCID: PMC2654152.
20. Mubaiwa TD, Hartley-Tassell LE, Semchenko EA, Jen FE, Srikhanta YN, Day CJ, et al. The glycointeractome of serogroup B *Neisseria meningitidis* strain MC58. *Scientific reports*. 2017; 7(1):5693. <https://doi.org/10.1038/s41598-017-05894-w> PMID: 28720847; PubMed Central PMCID: PMC5515891.
21. Shewell LK, Harvey RM, Higgins MA, Day CJ, Hartley-Tassell LE, Chen AY, et al. The cholesterol-dependent cytolytins pneumolysin and streptolysin O require binding to red blood cell glycans for hemolytic activity. *Proc Natl Acad Sci U S A*. 2014; 111(49):E5312–20. Epub 2014/11/26. <https://doi.org/10.1073/pnas.1412703111> PMID: 25422425; PubMed Central PMCID: PMC4267402.
22. Tromp AT, Van Gent M, Abrial P, Martin A, Jansen JP, De Haas CJC, et al. Human CD45 is an F-component-specific receptor for the staphylococcal toxin Pantone-Valentine leukocidin. *Nat Microbiol*. 2018; 3(6):708–17. Epub 2018/05/08. <https://doi.org/10.1038/s41564-018-0159-x> PMID: 29736038.
23. Corcionivoschi N, Alvarez LA, Sharp TH, Strengert M, Alemka A, Mantell J, et al. Mucosal reactive oxygen species decrease virulence by disrupting *Campylobacter jejuni* phosphotyrosine signaling. *Cell Host Microbe*. 2012; 12(1):47–59. Epub 2012/07/24. <https://doi.org/10.1016/j.chom.2012.05.018> PMID: 22817987; PubMed Central PMCID: PMC3749511.
24. Funderburgh JL. Keratan sulfate: structure, biosynthesis, and function *Glycobiology* 2000; 10(10):951–8. <https://doi.org/10.1093/glycob/10.10.951> PMID: 11030741.
25. Goletz S, Hanisch FG, Karsten U. Novel alphaGalNAc containing glycans on cytokeatins are recognized invitro by galectins with type II carbohydrate recognition domains. *J Cell Sci* 1997; 110 (Pt 14):1585–96. PMID: 9247192.
26. Schafer IA, Sorrell JM. Human keratinocytes contain keratin filaments that are glycosylated with keratan sulfate. *Exp Cell Res* 1993; 207(2):213–9. <https://doi.org/10.1006/excr.1993.1185> PMID: 7688312.
27. Grant OC, Smith HM, Firsova D, Fadda E, Woods RJ. Presentation, presentation, presentation! Molecular-level insight into linker effects on glycan array screening data. *Glycobiology*. 2014; 24(1):17–25.

- Epub 2013/09/24. <https://doi.org/10.1093/glycob/cwt083> PMID: 24056723; PubMed Central PMCID: PMC3854501.
28. Lewallen DM, Siler D, Iyer SS. Factors affecting protein-glycan specificity: effect of spacers and incubation time. *Chembiochem* 2009; 10(9):1486–9. Epub 2009/05/28. <https://doi.org/10.1002/cbic.200900211> PMID: 19472251.
  29. Gagneux P, Cheriyian M, Hurtado-Ziola N, van der Linden EC, Anderson D, McClure H, et al. Human-specific regulation of alpha 2-6-linked sialic acids. *J Biol Chem*. 2003; 278(48):48245–50. Epub 2003/09/23. <https://doi.org/10.1074/jbc.M309813200> PMID: 14500706.
  30. van der Werf TS, van der Graaf WT, Tappero JW, Asiedu K. *Mycobacterium ulcerans* infection. *Lancet* 1999; 354(9183):1013–8. Epub 1999/09/29. [https://doi.org/10.1016/S0140-6736\(99\)01156-3](https://doi.org/10.1016/S0140-6736(99)01156-3) PMID: 10501380.
  31. Stanley P, Schachter H, Taniguchi N. N-Glycans. In: nd, Varki A, Cummings RD, Esko JD, Freeze HH, Stanley P, et al., editors. *Essentials of Glycobiology*. Cold Spring Harbor (NY)2009.
  32. Jin SP, Chung JH. Inhibition of N-glycosylation by tunicamycin attenuates cell-cell adhesion via impaired desmosome formation in normal human epidermal keratinocytes. *Bioscience reports*. 2018;38(6). <https://doi.org/10.1042/BSR20171641> PMID: 30291216; PubMed Central PMCID: PMC6259015.
  33. Kariya Y, Gu J. N-glycosylation of ss4 integrin controls the adhesion and motility of keratinocytes. *PLoS One* 2011; 6(11):e27084. <https://doi.org/10.1371/journal.pone.0027084> PMID: 22073258; PubMed Central PMCID: PMC3206902.
  34. Belotserkovsky I, Brunner K, Pinaud L, Rouvinski A, Dellarole M, Baron B, et al. Glycan-Glycan Interaction Determines Shigella Tropism toward Human T Lymphocytes. *mBio*. 2018; 9(1). Epub 2018/02/15. <https://doi.org/10.1128/mBio.02309-17> PMID: 29440574; PubMed Central PMCID: PMC5821077.
  35. Day CJ, Tran EN, Semchenko EA, Tram G, Hartley-Tassell LE, Ng PS, et al. Glycan:glycan interactions: High affinity biomolecular interactions that can mediate binding of pathogenic bacteria to host cells. *Proceedings of the National Academy of Sciences of the United States of America*. 2015; 112(52):E7266–75. Epub 2015/12/18. <https://doi.org/10.1073/pnas.1421082112> PMID: 26676578; PubMed Central PMCID: PMC4702957.
  36. Wang XQ, Sun P, Al-Qamari A, Paller AS. Gangliosides block keratinocyte binding to fibronectin through carbohydrate-carbohydrate binding to the alpha5 subunit of alpha5beta1. *J Invest Dermatol*. 2000; 115(2):333. Epub 2000/08/22. <https://doi.org/10.1046/j.1523-1747.2000.115002333.x> PMID: 10951263.
  37. Mikhalchik EV, Shiyan SD, Bovin NV. Carbohydrate-carbohydrate interaction: zymosan and beta-glucan from *Saccharomyces cerevisiae* bind mannoseylated glycoconjugates. *Biochemistry (Mosc)* 2000; 65(4):494–501. Epub 2000/05/16. PMID: 10810189
  38. Tran ENH, Day CJ, Poole J, Jennings MP, Morona R. Specific blood group antibodies inhibit *Shigella flexneri* interaction with human cells in the absence of spinoculation. *Biochem Biophys Res Commun* 2020; 521(1):131–6. Epub 2019/10/22. <https://doi.org/10.1016/j.bbrc.2019.10.091> PMID: 31630794.
  39. Semchenko EA, Everest-Dass AV, Jen FE, Mubaiwa TD, Day CJ, Seib KL. Glycointeractome of *Neisseria gonorrhoeae*: Identification of Host Glycans Targeted by the Gonococcus To Facilitate Adherence to Cervical and Urethral Epithelial Cells. *mBio*. 2019; 10(4). Epub 2019/07/11. <https://doi.org/10.1128/mBio.01339-19> PMID: 31289181; PubMed Central PMCID: PMC6747729.
  40. Hashish E, Merwad A, Elgaml S, Amer A, Kamal H, Elsadek A, et al. *Mycobacterium marinum* infection in fish and man: epidemiology, pathophysiology and management; a review. *Vet Q*. 2018; 38(1):35–46. Epub 2018/03/02. <https://doi.org/10.1080/01652176.2018.1447171> PMID: 29493404; PubMed Central PMCID: PMC6831007.
  41. Sette CS, Wachholz PA, Masuda PY, da Costa Figueira RB, de Oliveira Mattar FR, Ura DG. *Mycobacterium marinum* infection: a case report. *J Venom Anim Toxins Incl Trop Dis*. 2015; 21:7. Epub 2015/03/26. <https://doi.org/10.1186/s40409-015-0008-9> PMID: 25806076; PubMed Central PMCID: PMC4372314.
  42. Johnson MG, Stout JE. Twenty-eight cases of *Mycobacterium marinum* infection: retrospective case series and literature review. *Infection*. 2015; 43(6):655–62. Epub 2015/04/15. <https://doi.org/10.1007/s15010-015-0776-8> PMID: 25869820; PubMed Central PMCID: PMC6535045.
  43. Slany M, Jezek P, Bodnarova M. Fish tank granuloma caused by *Mycobacterium marinum* in two aquarists: two case reports. *Biomed Res Int*. 2013; 2013:161329. Epub 2014/01/07. <https://doi.org/10.1155/2013/161329> PMID: 24392446; PubMed Central PMCID: PMC3874340.
  44. Arima K, Fujita H, Toita R, Imazu-Okada A, Tsutsumishita-Nakai N, Takeda N, et al. Amounts and compositional analysis of glycosaminoglycans in the tissue of fish. *Carbohydr Res*. 2013; 366:25–32. Epub 2012/12/25. <https://doi.org/10.1016/j.carres.2012.11.010> PMID: 23261779.
  45. Souza AR, Kozlowski EO, Cerqueira VR, Castelo-Branco MT, Costa ML, Pavao MS. Chondroitin sulfate and keratan sulfate are the major glycosaminoglycans present in the adult zebrafish *Danio rerio*

- (Chordata-Cyprinidae). Glycoconj J 2007; 24(9):521–30. Epub 2007/06/02. <https://doi.org/10.1007/s10719-007-9046-z> PMID: 17541818.
46. Pfeiler E. Isolation and partial characterization of a novel keratan sulfate proteoglycan from metamorphosing bonefish (*Albula*) larvae. Fish Physiol Biochem 1988; 4(4):175–87. Epub 1988/01/01. <https://doi.org/10.1007/BF01871744> PMID: 24226299.
  47. Moll R, Divo M, Langbein L. The human keratins: biology and pathology. Histochem Cell Biol 2008; 129(6):705–33. <https://doi.org/10.1007/s00418-008-0435-6> PMID: 18461349; PubMed Central PMCID: PMC2386534.
  48. Sorrell JM, Caterson B, Caplan AI, Davis B, Schafer IA. Human keratinocytes contain carbohydrates that are recognized by keratan sulfate-specific monoclonal antibodies. J Invest Dermatol 1990; 95(3):347–52. Epub 1990/09/01. <https://doi.org/10.1111/1523-1747.ep12485110> PMID: 1696604.
  49. Chakravarti S, Magnuson T, Lass JH, Jepsen KJ, LaMantia C, Carroll H. Lumican regulates collagen fibril assembly: skin fragility and corneal opacity in the absence of lumican. J Cell Biol 1998; 141(5):1277–86. <https://doi.org/10.1083/jcb.141.5.1277> PMID: 9606218; PubMed Central PMCID: PMC2137175.
  50. Yeh JT, Yeh LK, Jung SM, Chang TJ, Wu HH, Shiu TF, et al. Impaired skin wound healing in lumican-null mice. The British journal of dermatology. 2010; 163(6):1174–80. <https://doi.org/10.1111/j.1365-2133.2010.10008.x> PMID: 20738297.
  51. Knobel M, O'Toole EA, Smith FJ. Keratins and skin disease. Cell Tissue Res 2015; 360(3):583–9. <https://doi.org/10.1007/s00441-014-2105-4> PMID: 25620412.
  52. Vasconcelos A, Cavaco-Paulo A. The use of keratin in biomedical applications. Curr Drug Targets 2013; 14(5):612–9. <https://doi.org/10.2174/1389450111314050010> PMID: 23410124.